

# Unsupervised Feature Disentanglement and Augmentation Network for One-class Face Anti-spoofing

Pei-Kai Huang, Jun-Xiong Chong, Ming-Tsung Hsu, Fang-Yu Hsu, Yi-Ting Lin, Kai-Heng Chien, Hao-Chiang Shao<sup>†</sup>, *Member, IEEE*, Chiou-Ting Hsu, *Senior Member, IEEE*

**Abstract**—Face anti-spoofing (FAS) techniques aim to enhance the security of facial identity authentication by distinguishing authentic live faces from deceptive attempts. While two-class FAS methods risk overfitting to training attacks to achieve better performance, one-class FAS approaches handle unseen attacks well but are less robust to domain information entangled within the liveness features. To address this, we propose an Unsupervised Feature Disentanglement and Augmentation Network (UFDANet), a one-class FAS technique that enhances generalizability by augmenting face images via disentangled features. The UFDANet employs a novel unsupervised feature disentangling method to separate the liveness and domain features, facilitating discriminative feature learning. It integrates an out-of-distribution liveness feature augmentation scheme to synthesize new liveness features of unseen spoof classes, which deviate from the live class, thus enhancing the representability and discriminability of liveness features. Additionally, UFDANet incorporates a domain feature augmentation routine to synthesize unseen domain features, thereby achieving better generalizability. Extensive experiments demonstrate that the proposed UFDANet outperforms previous one-class FAS methods and achieves comparable performance to state-of-the-art two-class FAS methods.

**Index Terms**—Face anti-spoofing, one-class classification, disentangled feature learning, affine feature transformation, adversarial feature learning.

## I. INTRODUCTION

Face anti-spoofing (FAS) aims to distinguish spoof faces from live ones to enhance the security of facial identification systems. Many face anti-spoofing methods [1]–[4] have been proposed to employ the two-class classification method, learning discriminative feature characteristics from both live and spoof images to counter various spoofing attacks. While two-class FAS methods perform well in detecting spoof attacks covered by training domain data, they often fail to identify unseen spoof attacks from out-of-distribution (OOD) testing domains during inference. In contrast, one-class FAS approaches [5]–[8] can be robust against the OOD problem by learning liveness information solely from live images. However, learning solely from live images implies acquiring features entwined with both liveness and domain information.

Note that, liveness information refers to the ability to distinguish real faces from facial spoof representations (e.g., photos, videos, or masks) in FAS, while domain information impacts model generalization by reflecting characteristics specific to different data distributions, involving variations in environment conditions or camera devices. Liveness and domain features naturally involve liveness and domain information in the latent spaces, respectively. Consequently, one-class FAS approaches tend to exhibit sensitivity to domain information and reduced generalizability against unseen attacks. Moreover, relying exclusively on live images renders one-class FAS approaches less competitive compared to two-class methods. To address these challenges, we propose a framework in this paper to augment liveness features, which are disentangled from the live images, with additional domain information. The proposed framework aims to create a training set with more discriminative and generalized features, thereby enhancing the effectiveness of one-class FAS approaches.

Recently, many two-class FAS methods have leveraged both live and spoof training images, adopting supervised disentangled feature learning [9]–[13] and various augmentation strategies [4], [12], [14] to counter spoof attacks such as Print Attacks (i.e., displaying printed faces on paper), Replay Attacks (i.e., replaying face videos on digital devices), and 3D Mask Attacks (i.e., wearing 3D masks). In general, facial spoof attacks encompass various attack types and often entail significant distribution discrepancies between training and testing domains, making it challenging to learn a compact feature space from spoof attacks [15]. Additionally, live faces are typically collected from real individuals and generally exhibit minor distribution discrepancies across training and test domains [15]. FAS models are more feasible for learning liveness features from live images, as these features are crucial for distinguishing live faces from spoof attacks. Since images captured under different environmental conditions often contain varying domain information, liveness features may become entangled with live/spoof-irrelevant domain features, leading to model degradation. Hence, some two-class FAS methods [9]–[13] typically employ supervised disentangled feature learning, which leverages live/spoof samples along with corresponding binary live/spoof labels and domain labels to separate liveness and domain features from mixed representations, thereby enhancing the model’s generalization ability. These supervised disentangled feature learning methods use the disentangled liveness features to distinguish live faces from

Manuscript submitted XX, XX, 2024.

H.-C. Shao (shao.haochiang@gmail.com) is the corresponding author with the Institute of Data Science and Information Computing, National Chung Hsing University, Taichung City 402204, Taiwan.

P.-K. Huang, J.-X. Chong, M.-T. Hsu, and F.-Y. Hsu are the students at the Department of Computer Science, National Tsing Hua University, Taiwan.

C.-T. Hsu is currently a Professor at the Department of Computer Science, National Tsing Hua University, Taiwan.

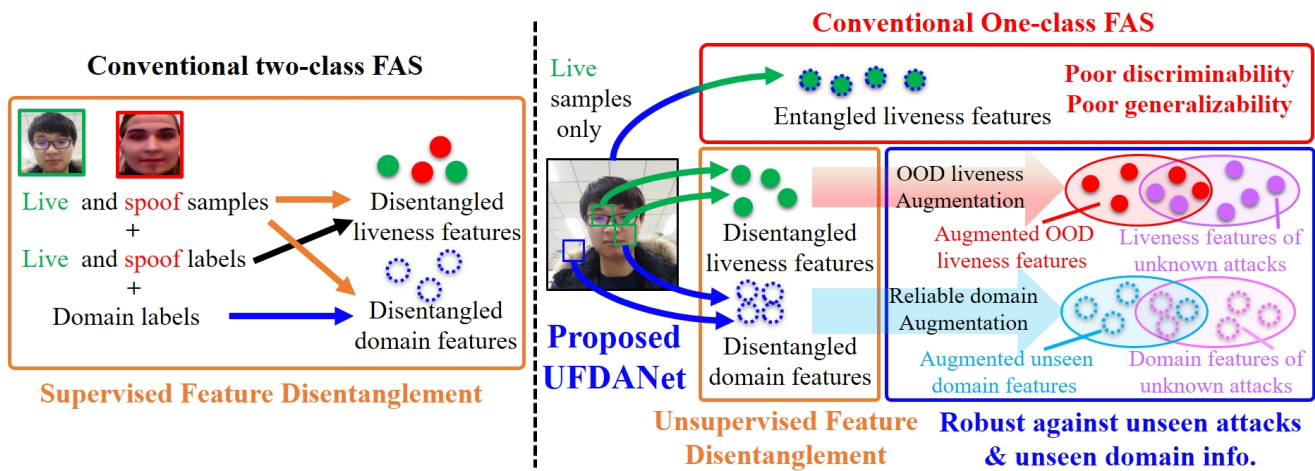


Fig. 1. Design concept of the proposed UFDANet. Existing two-class FAS methods adopt **supervised feature disentanglement** by using live and spoof samples, binary live/spoof labels, and domain labels to disentangle liveness and domain features for enhancing the generalization ability of FAS models. However, due to the absence of spoof samples/labels and domain labels, conventional one-class FAS methods that overlook domain information and extract liveness features entangled with domain features, which leads to poor generalizability and discriminability. To address this issue in one-class FAS, we propose a novel UFDANet. Since foreground facial regions share similar liveness information, while foreground facial regions and background non-facial regions exhibit similar domain information for the same live sample, UFDANet first aims to disentangle liveness and domain features in an **unsupervised patchwise manner** from live samples only. Next, we adopt the disentangled liveness and domain features to: i) synthesize the out-of-distribution (OOD) live features to augment absent spoof class samples and ii) generate unseen domain features to augment spoof samples, thereby enhancing the OOD generalizability of one-class FAS.

spoof attacks, as shown in Fig. 1. To further enhance the domain generalization ability of FAS models, these supervised feature disentanglement-based methods suggest swapping or remixing the disentangled liveness and domain features to augment the training data. Although this disentangling-and-swapping process increases the amount of training data, the augmented data still carry the same liveness and domain information from the source training domains. Since no out-of-domain information is introduced into the training process, the model’s feature representability remains limited. To address this issue, recent two-class FAS methods have proposed various augmentation strategies, such as color jitter and color masking [4], feature mixing [14], and diverse/unseen feature augmentation [12]. These approaches aim to improve discriminability by enriching the liveness features in the latent space. Inspired by the success of the aforementioned two-class FAS methods that leverage **supervised** disentangled feature learning and various augmentation strategies, in this paper, we aim to disentangle liveness and domain features in an **unsupervised** manner and subsequently augment them to enhance the discriminability and generalizability of the one-class FAS model.

In contrast to two-class methods, one-class FAS methods [5]–[8], [16], which learn only from live images, are free from overfitting to specific attacks; however, they still face three major challenges. First, similar to one-class anomaly detection and novelty detection techniques, one-class FAS methods struggle to effectively learn the abstract concepts of ‘live’ and ‘spoof,’ making it difficult to distinguish between live and spoof images. Second, unlike other one-class classification applications [17], [18], where significant visual differences generally exist between normal training data and target abnormal samples, the one-class FAS task must handle

data with highly similar visual characteristics between live and spoof faces. This similarity poses a second challenge: it is difficult for one-class FAS methods to learn discriminative liveness features and distinguish live faces from spoof ones based solely on visual cues from live images. Third, the final challenge arises from learning with entangled features. While two-class FAS methods [9]–[13] employ supervised disentangled feature learning, using live/spoof and domain labels to separate liveness and domain features and improve model generalizability, this strategy is not applicable to one-class FAS methods due to the absence of spoof images in the training data. As a result, the liveness features learned by previous one-class FAS methods [5]–[8], [16] are susceptible to domain information and may overfit to the training domains, as shown in Fig. 1. Therefore, compared to existing one-class FAS methods [5]–[8], [16], which may suffer and degrade due to unseen domain information, we first focus on learning the disentangled liveness features to mitigate the interference of domain information. Next, although the authors in [16] proposed using non-zero spoof cue maps to generate pseudo latent spoof features, they overlooked the influence of unknown domain information for one-class FAS models. Our approach addresses this gap by disentangling domain information and augmenting unseen domain features to contain authentic real-world domain characteristics, thereby enhancing the generalizability and robustness of one-class FAS models. We next describe the details of our approach.

In this paper, we propose a novel Unsupervised Feature Disentanglement and Augmentation Network (**UFDANet**) to address the aforementioned three challenges. Fig. 1 illustrates the core concept of our approach. First, to address the issue of entangled feature learning within one-class FAS, we propose an unsupervised feature disentanglement method to

separate domain and liveness features from live images. Specifically, building on the observation that different facial and non-facial regions from the same video share similar domain information [19], we propose to disentangle the domain features common to both facial and non-facial regions within the same live image. Additionally, based on the widely accepted assumption that different facial regions from the same video share similar liveness information [20], we further disentangle the liveness features from various facial regions within the same live image. **Second, to overcome the challenge of one-class data, which makes it difficult for one-class FAS models to learn the abstract concepts of ‘live’ and ‘spooof’ and effectively distinguish between live and spooof faces sharing highly similar visual characteristics, we propose an out-of-distribution (OOD) liveness feature augmentation scheme to synthesize OOD liveness features for the absent spooof class.** To generate these OOD liveness features, we adopt our previously proposed affine feature transformation layer from [12] to transfer the liveness features away from the genuine class. Simultaneously, to explore the latent space for unseen spooof-class liveness features, we employ a fixed-size memory bank to store sufficiently independent liveness features, thereby closely approximating the global latent feature space. **Third, to address unseen domain information and enhance representation capability beyond the training domains, we propose a reliable domain feature augmentation strategy to ensure that the generated domain features capture unseen and real-world domain information.** Specifically, we introduce a novel Generative Instance Normalization Encoder, utilizing a condition generator in conjunction with our previously proposed learnable Adaptive Instance Normalization (AdaIn) layer from [12] to generate a large number of unseen domain features. Additionally, we develop a reliable adversarial domain learning mechanism to guarantee that the augmented unseen domain features contain authentic real-world domain characteristics. To evaluate the effectiveness of the proposed **UFDANet**, we conduct extensive experiments on eight public face anti-spoofing datasets. The experimental results from both intra-domain and cross-domain testing demonstrate that **UFDANet** not only outperforms previous one-class FAS methods across most evaluation protocols but also achieves competitive performance when compared to state-of-the-art two-class FAS methods.

The main contributions of this paper are listed as follows.

- To address the issue that one-class FAS methods are often too domain-sensitive to detect unseen attacks during inference, we propose an Unsupervised Feature Disentanglement and Augmentation Network (**UFDANet**) capable of augmenting disentangled domain-agnostic features. Extensive experiments demonstrate the effectiveness of the proposed **UFDANet**.
- **To address the issue of entangled feature learning in one-class FAS**, we propose an unsupervised feature disentanglement scheme that separates liveness and domain features from live images.
- **To overcome the challenge of one-class data**, we design an out-of-distribution (OOD) liveness feature augmenta-

tion scheme to synthesize new liveness features of unseen spooof classes, which deviate from the live class, thereby enhancing the representability and discriminability of liveness features in a one-class FAS scenario.

- **To expand the representation capability away from the training domains**, we propose a reliable domain feature augmentation scheme to synthesize unseen domain features containing real-world domain information, thereby further improving the generalizability of **UFDANet**.

## II. RELATED WORK

### A. Two-class Face Anti-Spoofing

1) *Methods involving Supervised Disentangled Feature Learning*: Several two-class FAS methods [9]–[13] have proposed using live/spooof and domain labels to learn disentangled liveness features, aiming to reduce the interference of domain information and effectively distinguish between live and spooof images. Zhang *et al.* pioneered the use of supervised disentangled feature learning to improve face anti-spoofing under the intra-domain scenario [9]. Building on this, Wang *et al.* and Wang *et al.* introduced approaches to disentangle liveness features from identity/domain features across different domains and remix them to enhance FAS models [10], [11]. However, since training datasets often consist of limited subjects and small variations of attacks, the disentangled liveness features may not generalize well to unseen domains. To address this, Wu *et al.* employed a generative model to increase the number of subjects, thus promoting better disentangled feature learning for face anti-spoofing [13]. Recently, Huang *et al.* proposed enriching the diversity of liveness features and expanding domain features to encompass a broader range of representation attacks, leading to improved generalization to unseen domains [12]. **In [21], Yue *et al.* proposed use using live/spooof and domain labels to disentangle liveness and subject features, and to reconstruct these features at the image level. Although the aforementioned two-class FAS methods adopt supervised disentangled feature learning using live/spooof samples along with corresponding binary labels and domain labels to enhance the generalization ability of FAS models, these approaches cannot be applied to one-class FAS due to the absence of spooof data, spooof labels, and domain labels.**

2) *Methods involving Data Augmentation*: In recent years, researchers have proposed various augmentation strategies to enhance the generalization ability of FAS models and face classification models. For example, Shao *et al.* developed a domain-transfer face augmentation network that decomposes a face image into disentangled attribute components—such as an identity feature, a pose and expression feature, a lighting feature, and a general feature—allowing for the synthesis of new face images of the same individual by manipulating other three components [22]. Huang *et al.* introduced a feature mixing augmentation technique that blends specific feature statistics from different domains to promote the learning of domain-invariant features [14]. Building on this, Wang *et al.* proposed a negative data augmentation scheme utilizing

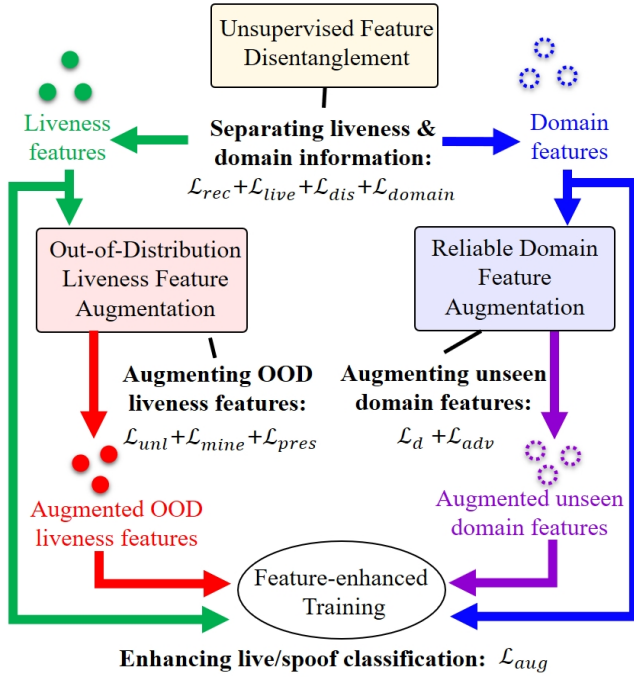


Fig. 2. Overview of the proposed proposed unsupervised disentangled feature augmentation network (UFDANet), which includes three key modules: i) an unsupervised feature disentanglement module that separates liveness and domain features, ii) an out-of-distribution (OOD) liveness feature augmentation module for synthesizing absent spoof classes, and iii) a reliable domain feature augmentation module for generating reliable, unseen domain features. The augmented OOD liveness and unseen domain features are combined to enhance live and spoof classification.

color jitter and color masking to simulate unseen domain information, effectively addressing a wide range of attacks in real-world scenarios [4]. However, spoof data generated solely through color jitter and color masking offers limited domain variability. To address this limitation, Huang *et al.* [12] enriched the diversity of disentangled liveness features and expanded domain features, thereby improving generalization to unseen domains. While previous two-class face anti-spoofing methods have achieved promising results through disentangled feature learning, most of these approaches depend heavily on labeled live and spoof data, along with domain labels, to effectively perform the feature disentanglement process.

### B. One-class Face Anti-Spoofing

One-class FAS methods focus on learning liveness features exclusively from live images to differentiate live images from spoof images. Lim *et al.* [8] and Huang *et al.* [7] proposed reconstructing facial content to capture liveness information. However, due to the absence of spoof faces, these FAS models may tend to learn general facial features rather than true liveness features. Additionally, Nikisins *et al.* [5] and Baweja *et al.* [6] suggested using Gaussian Mixture Models (GMMs) to learn liveness features from live images. Specifically, Nikisins *et al.* used the Image Quality Measures introduced in [23] to model the GMM distribution of live images, while Baweja *et al.* mixed noise sampled from a Gaussian distribution with liveness features from live images to generate pseudo spoof

features. Nevertheless, since live images lack spoof cues, Huang *et al.* proposed using non-zero spoof cue maps to generate pseudo latent spoof features to enhance the learning process for one-class FAS methods [16]. However, the performance metrics, such as ACER [24], of one-class FAS methods are still not competitive with two-class FAS methods, indicating that there remains a need to design mechanisms to improve one-class FAS approaches. As shown in Figure 1, existing one-class FAS methods [5]–[8], [16] overlook domain information and extract liveness features that are entangled with domain features, resulting in poor generalizability and discriminability. Hence, the proposed method first focuses on learning disentangled liveness and domain features to reduce the influence of live/spoof-irrelevant domain information. In addition, previous one-class FAS methods adopt various strategies, such as reconstructing faces [7], [8] or using Gaussian Mixture Models (GMMs) [5], [6] to learn liveness features. In contrast, we propose augmenting out-of-distribution (OOD) samples to focus on learning liveness features solely from live samples, enhancing the discriminability of FAS models to distinguish live faces from unknown spoof attacks. Unlike previous one-class FAS methods that overlook the interference of domain information, we further augment unseen domain features to enhance the generalization ability of FAS models.

## III. UNSUPERVISED FEATURE DISENTANGLEMENT AND AUGMENTATION NETWORK (UFDANET)

### A. Overview

The proposed UFDANet (Unsupervised Feature Disentanglement and Augmentation Network) addresses the challenge faced by one-class face anti-spoofing (FAS) methods whose training dataset contains only live face images. This limitation necessitates a model capable of effectively detecting out-of-distribution (OOD) occurrences during inference, including unseen spoof attacks and samples with novel domain features. To this end, as shown in Fig. 2, UFDANet introduces three key components. First, we propose an **unsupervised feature disentanglement** process to separate liveness and domain information. Unlike previous one-class FAS methods, which learn entangled liveness features sensitive to domain-related factors, our disentanglement mitigates this influence to improve model’s robustness. Second, the **OOD liveness feature augmentation** module adopts the disentangled liveness features of live samples to synthesize liveness features for absent spoof classes, enabling anti-spoof detection for OOD spoof samples. Third, the **reliable domain feature augmentation** module generates reliable unseen domain features to enrich the training dataset with diverse and challenging cases, enhancing the model’s domain generalizability. Finally, we use the augmented OOD liveness and unseen domain features to enhance FAS model training for improving the discrimination between live and spoof samples. Each of these components will be detailed in the following subsections. Fig. 3 presents the flow diagram of UFDANet, while Table I summarizes the notations used throughout this paper.

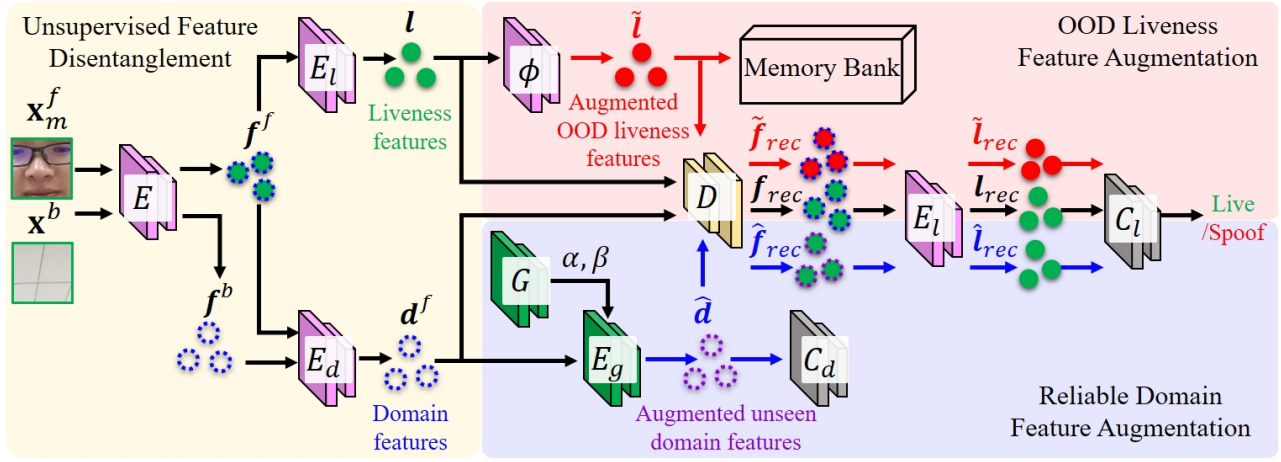


Fig. 3. Flow diagram of UFDANet. Dotted circles represent domain features, e.g.  $d^f$  and  $\hat{d}$ . Solid circles denote liveness features, e.g.  $l$  and  $\tilde{l}$ . Solid circles with dashed outer borders indicate liveness features infused with domain information, e.g.  $f^f$  and  $\tilde{f}_{rec}$ .

TABLE I  
SUMMARY OF NOTATIONS

Symbol	Definition
$x$	The live image for training.
$x^f$	The foreground facial part of $x$ .
$x^b$	The background non-facial part of $x$ .
$x_m^f$	The patch obtained via random masking of $x^f$ .
$E(\cdot)$	The general feature encoder.
$E_l(\cdot)$	The liveness feature extractor.
$E_d(\cdot)$	The domain feature extractor.
$D(\cdot)$	The general feature reconstructor.
$\phi(\cdot)$	The OOD liveness feature synthesizer.
$E_{GIN}$	The GIN encoder for domain feature augmentation.
$G$	The condition generator for producing affine parameters, i.e., $(\alpha, \beta)$ , required by $E_{GIN}$ .
$f^f$	$f^f = E(x_m^f)$ , the general feature of $x_m^f$ .
$f^b$	$f^b = E(x^b)$ , the general feature of $x^b$ .
$l$	$l = E_l(f^f)$ , the liveness feature extracted from $f^f$ .
$d^f$	$d^f = E_d(f^f)$ , the domain feature carried by $f^f$ .
$d^b$	$d^b = E_d(f^b)$ , the domain feature carried by $f^b$ .
$\tilde{f}_{rec}$	The general feature reconstructed by $\tilde{f}_{rec} = D(l, d^f)$ .
$l_{rec}$	The liveness feature extracted from $\tilde{f}_{rec}$ by $E_l(\cdot)$ .
$\tilde{l}$	$\tilde{l} = \phi(l)$ , the augmented OOD liveness feature.
$\tilde{l}_B$	The $\tilde{l}$ 's stored in the memory bank $B$ .
$\tilde{f}_{rec}$	$\tilde{f}_{rec} = D(\tilde{l}, d^f)$ , the general feature reconstructed based on the augmented liveness feature $\tilde{l}$ .
$\tilde{l}_{rec}$	The liveness feature extracted from $\tilde{f}_{rec}$ by $E_l(\cdot)$ .
$\hat{d}$	$\hat{d} = E_{GIN}(d)$ , the augmented domain feature.
$\hat{f}_{rec}$	$\hat{f}_{rec} = D(l, \hat{d})$ , the general feature reconstructed based on the augmented domain feature $\hat{d}$ .
$\hat{l}_{rec}$	The liveness feature extracted from $\hat{f}_{rec}$ by $E_l(\cdot)$ .

### B. Module-1: Unsupervised Feature Disentanglement

While two-class FAS methods can learn to extract liveness and domain features separately from live and spoof training samples [9], [10], [12], [25], one-class FAS strategies face challenges caused by the absence of spoof images and corresponding domain information in their training datasets. This absence makes it difficult for one-class FAS techniques to mitigate the feature entanglement problem. To address this challenge, we propose a novel **unsupervised feature disentanglement (UFD)** method to separate liveness and domain

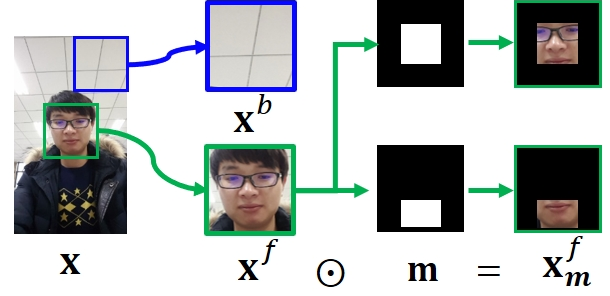


Fig. 4. Conceptual illustration of patchwise disentanglement of domain and liveness information within a live image. First, the foreground facial part,  $x^f$ , and the background non-facial part,  $x^b$ , should share the same domain information. Second, different masked facial areas,  $x_m^f$ , should contain the same liveness information. Consequently, the liveness and domain features can be distilled separately in a patchwise manner.

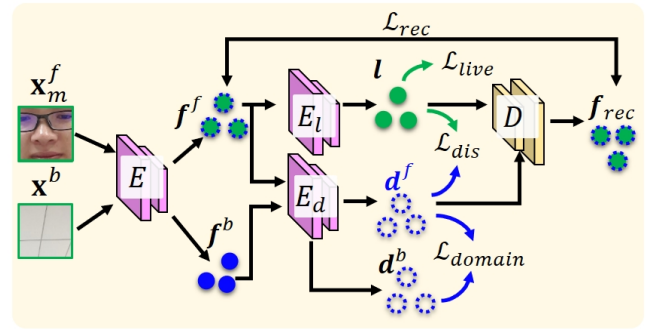


Fig. 5. Design of the proposed unsupervised feature disentanglement module. It consists of a general feature encoder  $E$ , a liveness feature extractor  $E_l$ , a domain feature extractor  $E_d$ , and a general feature reconstructor  $D$ , and it is driven by four loss terms:  $\mathcal{L}_{rec}$ ,  $\mathcal{L}_{live}$ ,  $\mathcal{L}_{dis}$ , and  $\mathcal{L}_{domain}$ .

features from live images, in one-class FAS scenarios lacking spoof images and domain labels.

The design of UFD method is inspired by two key data properties. First, in a training live image, the foreground facial part  $x^f$  and the background scene  $x^b$  generally share the same domain information because a facial video is typically

filmed by a single camera in a consistent environment [19]. Therefore, there should be a substantial overlap between the domain information carried by  $\mathbf{x}^f$  and  $\mathbf{x}^b$ , as illustrated in Fig. 4. Second, different patches of the same face  $\mathbf{x}_m^f$  within a video should have similar liveness features [20]. Consequently, based on these two properties, the proposed UFD method aims to separately extract i) the liveness feature  $\mathbf{l}$ , which is carried by different foreground facial parts  $\mathbf{x}_m^f$  of the live image  $\mathbf{x}$ ; and ii) the domain information carried by the foreground facial area  $\mathbf{x}^f$  and the background non-facial region  $\mathbf{x}^b$ .

As shown in Fig. 5, the proposed UFD method is driven by four loss terms, namely, i) the domain extraction loss  $\mathcal{L}_{domain}$ , ii) the liveness extraction loss  $\mathcal{L}_{live}$ , iii) feature disentanglement loss  $\mathcal{L}_{dis}$ , and iv) the reconstruction loss  $\mathcal{L}_{rec}$ . The domain extraction loss ensures consistency between the domain features extracted from the foreground part  $\mathbf{x}^f$  and the background part  $\mathbf{x}^b$ . Specifically, we define the domain extraction loss  $\mathcal{L}_{domain}$  to constrain the general feature encoder  $E$  and the domain feature extractor  $E_d$  by,

$$\mathcal{L}_{domain}(\theta_E, \theta_{E_d}) = \mathbb{E}\{1 - \cos(\mathbf{d}^f, \mathbf{d}^b)\}, \quad (1)$$

where  $\theta_E$  and  $\theta_{E_d}$  are the parameters of  $E$  and  $E_d$ , respectively,  $\mathbb{E}\{\cdot\}$  denotes the expectation, and  $\cos(\cdot, \cdot)$  represents the cosine similarity. Here,  $\mathbf{d}^f = E_d(E(\mathbf{x}_m^f))$  and  $\mathbf{d}^b = E_d(E(\mathbf{x}^b))$  correspond to the domain features extracted from the foreground facial part and the background part of a live image  $\mathbf{x}$ , respectively. Additionally,  $E(\cdot)$  refers to the general feature extractor used to derive the general feature, in which the domain information and liveness information are entangled, and  $E_d(\cdot)$  denotes the domain feature extractor. Note that  $\mathbf{x}_m^f = \mathbf{x}^f \odot \mathbf{m}$  represents the masked foreground facial patch obtained from  $\mathbf{x}^f$  via the mask  $\mathbf{m}$ , as already illustrated in Fig. 4.

Next, to facilitate the extraction of consistent liveness information from different masked foreground facial regions within the same live image  $\mathbf{x}$ , the liveness extraction loss  $\mathcal{L}_{live}$  is defined to constrain the general feature encoder  $E$  and the liveness feature extractor  $E_l$  by :

$$\mathcal{L}_{live}(\theta_E, \theta_{E_l}) = \mathbb{E}\{1 - \cos(\mathbf{l}_s, \mathbf{l}_t)\}, \quad (2)$$

where  $\theta_{E_l}$  denotes the parameters of  $E_l$ ,  $\mathbf{l}_s = E_l(E(\mathbf{x}_{m,s}^f))$  denotes the liveness feature extracted from the  $s$ -th masked foreground facial patch of  $\mathbf{x}^f$ , and  $E_l(\cdot)$  represents the liveness feature extractor.

Thirdly, the feature disentanglement loss  $\mathcal{L}_{dis}$  is designed to de-correlate the liveness feature and the domain feature extracted from the same masked facial part  $\mathbf{x}_m^f$ . This loss minimizes the cosine similarity between the extracted liveness and domain features, encouraging them to be orthogonal and thereby disentangled. Specifically, we define the feature disentanglement loss  $\mathcal{L}_{dis}$  to  $E$ ,  $E_l$ , and  $E_d$  by,

$$\mathcal{L}_{dis}(\theta_E, \theta_{E_l}, \theta_{E_d}) = \mathbb{E}\{\cos(\mathbf{l}_s, \mathbf{d}^f)\}. \quad (3)$$

Finally, we define the reconstruction loss  $\mathcal{L}_{rec}$  to constrain the general feature reconstructor  $D$  to reconstruct the general features  $\mathbf{f}^f$  by,

$$\mathcal{L}_{rec}(\theta_D) = \mathbb{E}\{\mathbf{f}^f - \mathbf{f}_{rec}\}. \quad (4)$$

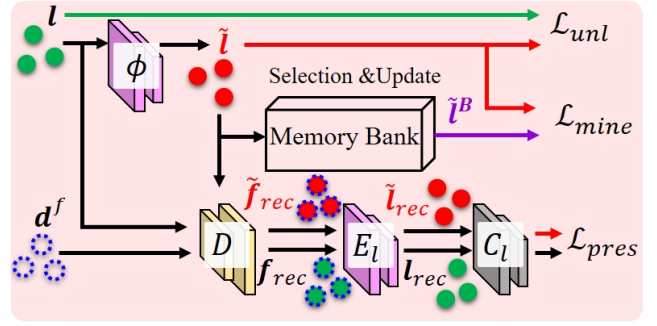


Fig. 6. Design of the proposed out-of-distribution (OOD) liveness feature augmentation module. In addition to the global feature decoder  $D$  and the liveness feature extractor  $E_l$ , this module incorporates three additional submodules: an OOD liveness feature adaptor  $\phi$ , a liveness classifier  $C_l$ , and a memory bank storing the augmented OOD liveness feature  $\tilde{\mathbf{l}}_B$ . It is driven by the unlikeness loss  $\mathcal{L}_{unl}$ , the liveness preservation loss  $\mathcal{L}_{pres}$ , and the OOD liveness mining loss  $\mathcal{L}_{mine}$ .

where  $\theta_D$  denotes the parameters of  $D$ . This loss ensures the accuracy of the extracted domain feature  $\mathbf{d}^f$  and liveness feature  $\mathbf{l}_s$  by minimizing the reconstruction error between i) the reconstructed global feature  $\mathbf{f}_{rec} = D(\mathbf{l}_s, \mathbf{d}^f)$  and ii) the global feature of the masked foreground facial image  $\mathbf{f}^f = E(\mathbf{x}_m^f)$ . Note that  $D(\cdot, \cdot)$  denotes a learnable general feature reconstructor, which will also be utilized in the later **OOD liveness feature augmentation and reliable domain feature augmentation** procedures. In summary, as shown in Fig. 5, we fixed the other modules while training  $E$ ,  $E_l$ ,  $E_d$ , and  $D$  to achieve the model training of the proposed unsupervised feature disentanglement by,

$$\theta_E^*, \theta_{E_l}^*, \theta_{E_d}^*, \theta_D^* = \arg \min_{\theta_E^*, \theta_{E_l}^*, \theta_{E_d}^*, \theta_D^*} (\mathcal{L}_{domain}(\theta_E, \theta_{E_d}) + \mathcal{L}_{rec}(\theta_D) + \mathcal{L}_{live}(\theta_E, \theta_{E_l}) + \mathcal{L}_{dis}(\theta_E, \theta_{E_l}, \theta_{E_d})). \quad (5)$$

### C. Module-2: Out-of-Distribution Liveness Feature Augmentation

Due to the absence of spoof information in the training dataset, one-class FAS methods often rely on out-of-distribution (OOD) detection strategies to identify spoofed images. Since a spoof attack typically involves factors other than human skin information [26], the spoofed samples usually reside far from the genuine class in the latent feature space. Consequently, to enhance the efficacy of one-class FAS methods, we develop an OOD liveness feature augmentation procedure. The main idea behind this procedure is to generate synthetic liveness features that diverge from those of the real live class. These OOD liveness features are then used to create a pseudo-spoof class, compensating for the lack of actual spoof attacks.

1) *Out-of-Distribution Liveness Feature Adaptor*: Inspired by the success of Feature-wise Transformation (FWT) on simulating diverse feature distributions [12], [27], we propose using the learnable affine feature transformation (AFT) to augment the liveness features of absent spoof class samples. Note that, unlike our previous work in [12], which diversifies live and spoof features in two-class FAS setting, we propose an OOD liveness feature augmentation using AFT to augment the liveness features of absent spoof class samples for one-class FAS.

The proposed OOD Liveness Feature Augmentation procedure operates primarily based on the OOD liveness feature adaptor  $\phi$ , as illustrated in Fig. 6. Given the liveness features  $\mathbf{l}_s$  extracted from the  $s$ -th masked foreground facial patch of  $\mathbf{x}^f$ , the OOD liveness feature adaptor  $\phi$  synthesizes an OOD liveness feature  $\tilde{\mathbf{l}}$  by

$$\tilde{\mathbf{l}}_s = \phi(\mathbf{l}_s) = \mathbf{s} \odot \text{Conv}(\mathbf{l}_s) + \mathbf{b}, \quad (6)$$

where  $\mathbf{s} \sim \mathcal{N}(1, \mathbf{s}_c)$  and  $\mathbf{b} \sim \mathcal{N}(0, \mathbf{b}_c)$  are sampled from learnable Gaussian distributions with learnable parameters  $\mathbf{s}_c$  and  $\mathbf{b}_c$ .

We design two loss terms for learning the OOD liveness feature adaptor  $\phi$  to ensure that the augmented OOD liveness feature can effectively create a pseudo-spoof class that is far from the genuine class. The first one is an unlikeness loss  $\mathcal{L}_{unl}$  encouraging the dissimilarity between the synthetic liveness feature  $\tilde{\mathbf{l}}_s$  and the input liveness feature  $\mathbf{l}_t$ . That is,

$$\mathcal{L}_{unl}(\theta_\phi) = \mathbb{E}\{\cos(\tilde{\mathbf{l}}_s, \mathbf{l}_t)\}. \quad (7)$$

The second is a liveness preservation loss  $\mathcal{L}_{pres}$  defined as

$$\mathcal{L}_{pres}(\theta_\phi) = -\mathbb{E}\{\log(C_l(\mathbf{l}_{rec})) + \log(1 - C_l(\tilde{\mathbf{l}}_{rec}))\}, \quad (8)$$

where  $C_l(\cdot)$  is the classifier for telling true liveness features apart from their augmented syntheses. Here,  $\mathbf{l}_{rec} = E_l(\mathbf{f}_{rec}) = E_l(D(\mathbf{l}, \mathbf{d}^f))$  denotes the liveness feature extracted from the reconstructed general feature, and  $\tilde{\mathbf{l}}_{rec} = E_l(\tilde{\mathbf{f}}_{rec}) = E_l(D(\tilde{\mathbf{l}}, \mathbf{d}^f))$  represents the one extracted from the general feature reconstructed from an augmented  $\tilde{\mathbf{l}}$ . Clearly, the liveness preservation loss is minimized when  $C_l(\mathbf{l}_{rec}) = 1$  and  $C_l(\tilde{\mathbf{l}}_{rec}) = 0$ . The former condition indicates that the liveness information carried by the augmented OOD liveness feature  $\tilde{\mathbf{l}}$  is distinguishable from  $\mathbf{l}$ , while the latter condition demonstrates that both the general feature reconstructor  $D(\cdot, \cdot)$  and the liveness feature extractor  $E_l(\cdot)$  function correctly, ensuring that the liveness information remains unaltered after the reconstruction and feature extraction procedures.

2) *Out-of-Distribution Liveness Feature Mining*: The OOD liveness feature mining scheme is designed to explore the latent feature space for potential spoof attacks, encouraging the OOD liveness feature adaptor  $\phi$  to effectively synthesize unseen OOD liveness features  $\tilde{\mathbf{l}} = \phi(\mathbf{l})$ . Utilizing a fixed-size memory bank  $\mathcal{B}$  that evolves a corresponding latent subspace, this scheme enables a more comprehensive exploration of the feature transformation process on a global scale. More specifically, for each training batch, an augmented OOD liveness feature  $\tilde{\mathbf{l}} = \phi(\mathbf{l})$  is added to the memory bank  $\mathcal{B}$  if the mean absolute cosine distance between  $\tilde{\mathbf{l}}$  and the features already stored in  $\mathcal{B}$  is smaller than a pre-defined threshold  $\delta$ , i.e.,  $\mathbb{E}\{|\cos(\tilde{\mathbf{l}}, \mathbf{l}_B)|\} < \delta, \forall \mathbf{l}_B \in \mathcal{B}$ . This ensures that the newly synthesized liveness feature is sufficiently independent of those already present in the memory bank. If  $\mathcal{B}$  is full, it will be updated using a first-in-first-out (FIFO) strategy. This updating routine aims to select a collection of liveness features  $\tilde{\mathbf{l}}_B$  that effectively covers the space where OOD liveness features reside, ensuring comprehensive representability.

Therefore, the OOD liveness feature mining loss  $\mathcal{L}_{mine}$  for this scheme is defined as

$$\mathcal{L}_{mine}(\theta_\phi) = -\mathbb{E}\left\{\log \frac{\exp(\cos(\tilde{\mathbf{l}}, \tilde{\mathbf{l}}_M))}{\exp(\cos(\tilde{\mathbf{l}}, \tilde{\mathbf{l}}_M)) + \sum_{\mathbf{l}_B \in \mathcal{B}} \exp(\cos(\tilde{\mathbf{l}}, \mathbf{l}_B))}\right\}, \quad (9)$$

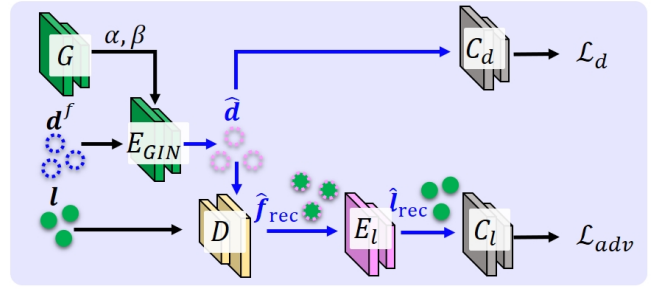


Fig. 7. Design of the proposed Domain Feature Augmentation module. Here,  $E_{GIN}$ ,  $G$ , and  $C_d$  denote respectively the Generative Instance Normalization (GIN) encoder, the conditional affine-parameter generator, and a domain classifier. Meanwhile,  $D$ ,  $E_l$ , and  $C_l$  are the same general feature reconstructor, liveness feature extractor, and liveness classifier shown in Figs. 5 and 6.

where  $\tilde{\mathbf{l}}_M$  denotes a randomly-masked version of the augmented OOD liveness feature  $\tilde{\mathbf{l}}$ , and thus  $(\tilde{\mathbf{l}}, \tilde{\mathbf{l}}_M)$  can be regarded as a positive pair.

To train the OOD liveness feature adaptor  $\phi$ , we fix the other modules and formulate the complete optimization problem for learning the parameters of  $\phi$  as follow:

$$\theta_\phi^* = \arg \min_{\theta_\phi} (\mathcal{L}_{unl}(\theta_\phi) + \mathcal{L}_{pres}(\theta_\phi) + \mathcal{L}_{mine}(\theta_\phi)). \quad (10)$$

In summary, the proposed OOD liveness feature adaptor is trained using three loss terms: i) the unlikeness loss  $\mathcal{L}_{unl}$ , ii) the liveness preservation loss  $\mathcal{L}_{pres}$ , and iii) the OOD liveness mining loss  $\mathcal{L}_{mine}$ . The first two loss terms ensure that  $\phi$  learns to generate OOD liveness features for the absent spoof class, while the third ensures that the synthetic OOD liveness features generated by  $\phi$  follow the distribution of the unseen spoof class in the latent space.

#### D. Module-3: Reliable Domain Feature Augmentation

Although our OOD liveness feature augmentation routine can synthesize a liveness feature  $\tilde{\mathbf{l}}$  for the pseudo-spoof class, all reconstructed global features  $\tilde{\mathbf{f}}_{rec} = D(\tilde{\mathbf{l}}, \mathbf{d}^f)$  still carry the same domain features as the training samples. This limits the representability of the reconstructed global feature to the source training domain. To address this, we propose a reliable domain feature augmentation scheme to enhance the representational capacity of features generated by UFDANet through the synthesis of unseen domain features. These synthetic domain features are intentionally designed to differ significantly from the training domain, thereby simulating potential real-world scenarios.

1) *Generative Instance Normalization*: Since Adaptive Instance Normalization (AdaIN) [28] adjusts feature styles to simulate diverse domains by adapting mean and variance statistics, in our previous work [12], we proposed a learnable AdaIN to cooperate with adversarial learning to generate unseen domain features. However, due to the lack of relevant constraints, the generated unseen domain features may deviate from real-world scenarios. Therefore, in this paper, we propose a reliable domain feature augmentation strategy to ensure that the synthesized domain features via learnable AdaIN faithfully capture the underlying characteristics of real-world data.

Fig. 7 illustrates the data flow of our reliable domain feature augmentation approach. This method primarily relies on a Generative Instance Normalization (GIN) encoder  $E_{GIN}(\cdot)$ , which incorporates a learnable Adaptive Instance Normalization (AdaIN) module [12] and a condition generator  $G$  for producing the affine parameters  $(\alpha, \beta)$ . This GIN encoder augments unseen domain features  $\hat{\mathbf{d}}$  by the following rule:

$$\hat{\mathbf{d}} = E_{GIN}(\mathbf{d}^f | G(\mathbf{n}_\alpha, \mathbf{n}_\beta)) = \alpha \cdot \left( \frac{\mathbf{d}^f - \mu_d}{\sigma_d} \right) + \beta. \quad (11)$$

Here,  $\mu_d$  and  $\sigma_d$  are the mean and standard deviation of domain feature  $\mathbf{d}^f$ , respectively; and,  $\alpha = G(\mathbf{n}_\alpha \parallel \mathbf{1})$  and  $\beta = G(\mathbf{n}_\beta \parallel \mathbf{2})$  represent the mean and standard deviation produced by  $G(\cdot)$  based on sampled Gaussian noise vectors  $\mathbf{n}_\alpha$  and  $\mathbf{n}_\beta$ , respectively. The symbol  $\parallel$  denotes vector concatenation, and  $\mathbf{1}$  and  $\mathbf{2}$  are both condition vectors.

This GIN routine samples different  $\alpha$  and  $\beta$  values from the learned distribution of the *unseen domain* to generate unseen domain features, rather than learning fixed constant  $\alpha$  and  $\beta$  values, as done in AdaIN [12]. In the next subsection, we will explore how the proposed GIN routine is encouraged to learn the distribution of the unseen domain features  $\hat{\mathbf{d}}$ .

2) *Reliable Adversarial Domain Learning*: To learn the distribution of  $\hat{\mathbf{d}}$ , the GIN encoder  $E_{GIN}(\cdot)$  guided by a reliable adversarial domain learning scheme we devised. This scheme addresses two practical concerns. The first is how to synthesize unseen domain features  $\hat{\mathbf{d}}$ , especially for domains not covered by the training data. The second focuses on how to ensure that the synthesized domain features faithfully capture the underlying characteristics of real-world data.

We design two loss terms to learn the Generative Instance Normalization (GIN) encoder  $E_{GIN}(\cdot)$  and the condition generator  $G$ . In particular, we tackle the first concern by defining an adversarial loss  $\mathcal{L}_{adv}$ . This loss encourages the liveness feature  $\hat{\mathbf{l}}_{rec} = E_l(\hat{\mathbf{f}}_{rec}) = E_l(D(\mathbf{l}, \hat{\mathbf{d}}))$ , which is extracted from the general feature reconstructed based on the unseen domain feature  $\hat{\mathbf{d}}$  and the liveness feature  $\mathbf{l}$  of the facial part, to deceive the liveness classifier  $C_l(\cdot)$ . Specifically, this loss is designed to encourage  $\hat{\mathbf{l}}_{rec}$  to fool the classifier  $C_l$ , i.e.,

$$\mathcal{L}_{adv}(\theta_G, \theta_{E_{GIN}}) = -\mathbb{E}\{\log(1 - C_l(\hat{\mathbf{l}}_{rec}))\}. \quad (12)$$

Additionally, because the unseen domain feature  $\hat{\mathbf{d}} = E_{GIN}(\mathbf{d})$  is synthesized by the GIN encoder, this adversarial loss  $\mathcal{L}_{adv}$  encourages the GIN encoder  $E_{GIN}$  to synthesize an unseen domain feature that is distinct from those learned by the liveness feature extractor  $E_l(\cdot)$ . However, merely encouraging the synthetic feature to be distinct from the training set features cannot guarantee that the augmented domain features carry real-world domain information. Therefore, we exploit an additional entropy loss  $\mathcal{L}_d$  to constrain  $E_{GIN}(\cdot)$  and  $G$  to resolve this issue. That is,

$$\mathcal{L}_d(\theta_G, \theta_{E_{GIN}}) = -\mathbb{E}\{\log(C_d(\hat{\mathbf{d}}))\}, \quad (13)$$

where  $C_d(\cdot)$  is a binary classifier pretrained with binary labels, where 1 indicates the domain feature and 0 indicates the liveness feature. This loss function ensures that the synthetic unseen domain feature  $\hat{\mathbf{d}}$  exhibits characteristics consistent

TABLE II  
DATASETS AND CORRESPONDING ABBREVIATIONS USED IN THIS PAPER

Dataset Name	Abb.	Dataset Name	Abb.
OULU-NPU [30]	<b>O</b>	MSU-MFSD [23]	<b>M</b>
CASIA-MFSD [31]	<b>C</b>	Idiap Replay-Attack [32]	<b>I</b>
SiW [33]	<b>S</b>	3DMAD [34]	<b>D</b>
HKBU-MARs [35]	<b>H</b>	CASIA-SURF [36]	<b>U</b>

with genuine domain features. The model training of reliable domain feature augmentation can be achieved with

$$\theta_G^*, \theta_{E_{GIN}}^* = \arg \min_{\theta_G^*, \theta_{E_{GIN}}^*} (\mathcal{L}_{adv}(\theta_G, \theta_{E_{GIN}}) + \mathcal{L}_d(\theta_G, \theta_{E_{GIN}})). \quad (14)$$

### E. Feature-enhanced Training

The representation capability of the proposed UFDANet is enhanced by the trained  $\phi$  and  $E_{GIN}$ . With the trained  $\phi$  and  $E_{GIN}$ , we first use  $\phi$  and  $E_{GIN}$  to synthesize the OOD liveness feature  $\tilde{\mathbf{l}}$  in Eq. (6) and to generate unseen domain features  $\hat{\mathbf{d}}$  in Eq. (11). Next, we reconstruct the augmented features  $\mathbf{f}_{rec} = D(\mathbf{l}_s, \mathbf{d}^f)$ ,  $\tilde{\mathbf{f}}_{rec} = D(\tilde{\mathbf{l}}, \mathbf{d}^f)$ , and  $\hat{\mathbf{f}}_{rec} = D(\mathbf{l}, \hat{\mathbf{d}})$ , and then extract the liveness features  $\mathbf{l}_{rec}$ ,  $\tilde{\mathbf{l}}_{rec}$ , and  $\hat{\mathbf{l}}_{rec}$  embedded within them to calculate the associated loss values. Finally, to enhance the model from the augmented features, we define the augmentation classification loss  $\mathcal{L}_{aug}$  to constrain the liveness classifier  $C_l(\cdot)$  and the liveness feature extractor  $E_l(\cdot)$  by,

$$\begin{aligned} \mathcal{L}_{aug}(\theta_{C_l}, \theta_{E_l}) &= -\mathbb{E}\{\log(C_l(\mathbf{l}_{rec}))\} - \mathbb{E}\{\log(1 - C_l(\tilde{\mathbf{l}}_{rec}))\} \\ &\quad - \mathbb{E}\{\log(C_l(\hat{\mathbf{l}}_{rec}))\}. \end{aligned} \quad (15)$$

Therefore, the model training of feature-enhanced training can be achieved with

$$\theta_{C_l}^*, \theta_{E_l}^* = \arg \min_{\theta_{C_l}^*, \theta_{E_l}^*} \mathcal{L}_{aug}(\theta_{C_l}, \theta_{E_l}). \quad (16)$$

### F. Training and testing

1) *Training*: We iteratively optimize the four coupled optimization problems of (5), (10), (14), and (16) in an alternate manner. In each iteration, we first update  $E$ ,  $E_l$ ,  $E_d$ , and  $D$  and fix other modules by minimizing  $\mathcal{L}_{domain}$ ,  $\mathcal{L}_{live}$ ,  $\mathcal{L}_{dis}$ , and  $\mathcal{L}_{rec}$  in Eq. (5). Next, we train  $\phi$  and fix other modules by minimizing  $\mathcal{L}_{uni}(\theta_\phi)$ ,  $\mathcal{L}_{pres}(\theta_\phi)$ , and  $\mathcal{L}_{mine}(\theta_\phi)$  in Eq. (10). Furthermore, we train  $G$  and  $E_{GIN}$  and fix other modules by minimizing  $\mathcal{L}_{adv}$  and  $\mathcal{L}_d$  in Eq. (14). Finally, we train  $C_l$  and  $E_l$  and fix other modules by minimizing  $\mathcal{L}_{aug}$  in Eq. (16). The detailed training process of UFDANet is provided in Algorithm 1.

2) *Testing*: During inference, each test image  $\mathbf{x}$  is classified based on the detection score  $s = C_l(E_l(E(\mathbf{x})))$ . Additionally, following previous methods [1], [11], we use the Youden Index Calculation [29] to derive the threshold for binary classification.

## IV. EXPERIMENTS

### A. Experiment Settings

1) *Datasets and Evaluation Metrics*: We evaluated the proposed UFDANet on eight face anti-spoofing datasets, including OULU-NPU [30], MSU-MFSD [23], CASIA-MFSD [31],



**Algorithm 1** Training of Unsupervised Feature Disentanglement and Augmentation Network (UFDANet)

**Input:**

$$\mathbf{x}_m^f, \mathbf{x}^b$$

**Initialization:**

Model parameters:  $\theta_E$  of  $E$ ,  $\theta_{E_l}$  of  $E_l$ ,  $\theta_{E_d}$  of  $E_d$ ,  $\theta_D$  of  $D$ ,  $\theta_\phi$  of  $\phi$ ,  $\theta_G$  of  $G$ ,  $\theta_{C_l}$  of  $C_l$ ,  $\theta_{E_{GIN}}$  of  $E_{GIN}$ .

- 1: **while** not done **do**
- 2:   # Unsupervised Feature Disentanglement
- 3:   Compute  $\mathcal{L}_{domain}(\theta_E, \theta_{E_d})$  by Eq. (1).
- 4:   Compute  $\mathcal{L}_{live}(\theta_E, \theta_{E_l})$  by Eq. (2).
- 5:   Compute  $\mathcal{L}_{dis}(\theta_E, \theta_{E_l}, \theta_{E_d})$  by Eq. (3).
- 6:   Compute  $\mathcal{L}_{rec}(\theta_D)$  by Eq. (4).
- 7:   Update  $\theta_E, \theta_{E_l}, \theta_{E_d}, \theta_D$  by Eq. (5).
- 8:   # OOD Liveness Feature Augmentation
- 9:   Synthesize the OOD liveness feature  $\tilde{l}$  by Eq. (6).
- 10:   Compute  $\mathcal{L}_{uni}(\theta_\phi)$  by Eq. (7).
- 11:   Compute  $\mathcal{L}_{pres}(\theta_\phi)$  by Eq. (8).
- 12:   Compute  $\mathcal{L}_{mine}(\theta_\phi)$  by Eq. (9).
- 13:   Update  $\theta_\phi$  by Eq. (10).
- 14:   # Reliable Domain Feature Augmentation
- 15:   Generate unseen domain features  $\tilde{d}$  by Eq. (11).
- 16:   Compute  $\mathcal{L}_{adv}(\theta_G, \theta_{E_{GIN}})$  by Eq. (12).
- 17:   Compute  $\mathcal{L}_d(\theta_G, \theta_{E_{GIN}})$  by Eq. (13).
- 18:   Update  $\theta_G, \theta_{E_{GIN}}$  by Eq. (14).
- 19:   # Feature-enhanced Training:
- 20:   Synthesize the OOD liveness feature  $\tilde{l}$  by Eq. (6).
- 21:   Generate unseen domain features  $\tilde{d}$  by Eq. (11).
- 22:   Reconstruct the augmented features  $\hat{\mathbf{f}}_{rec} = D(\tilde{l}, \tilde{d}^f)$ , and  $\hat{\mathbf{f}}_{rec} = D(\tilde{l}, \tilde{d})$
- 23:   Compute  $\mathcal{L}_{aug}(\theta_{C_l}, \theta_{E_l})$  by Eq. (15).
- 24:   Update  $\theta_{C_l}, \theta_{E_l}$  by Eq. (16).
- 25: **end while**
- 26: **return** Model parameters:  $\theta_E, \theta_{E_l}, \theta_{E_d}, \theta_D, \theta_\phi, \theta_G, \theta_{C_l}, \theta_{E_{GIN}}$

**Idiap Replay-Attack** [32], **SiW** [33], **3DMAD** [34], **HKBU-MARs** [35], and **CASIA-SURF** [36]. Table II provides the names and abbreviations of these datasets, which are referenced in subsequent discussions. To ensure fair comparisons with prior one-class and two-class methods, we adhered to the protocols established in previous studies [30], [33], [36], [37] for conducting intra-domain and cross-domain tests. The evaluation metrics used include: i) Attack Presentation Classification Error Rate (APCER) [24], ii) Bona Fide Presentation Classification Error Rate (BPCER) [24], iii) Average Classification Error Rate (ACER) [24], iv) Half Total Error Rate (HTER) [38], and v) Area Under the Curve (AUC).

*B. Ablation Study*

We conducted three sets of experiments to validate the contribution of each design component of UFDANet. Tables III, IV, and V present the ablation studies for its unsupervised feature disentanglement (Module-1), out-of-distribution (OOD) liveness feature augmentation (Module-2), and reliable domain feature augmentation (Module-3), respectively. In the following, we discuss these experiments in detail.

1) *Effectiveness of Unsupervised Feature Disentanglement:* In order to evaluate the efficacy of the loss terms designed for Module-1: unsupervised disentangled feature learning (*i.e.*,  $\mathcal{L}_{domain} + \mathcal{L}_{live} + \mathcal{L}_{dis} + \mathcal{L}_{rec}$ ), we assessed the performance gains achieved by two early FAS approaches, namely IQM-GMM [5] and Baweja et al.’s method [6], when trained with

TABLE III  
ABLATION STUDY ON THE PROTOCOL  $\mathbf{C} \rightarrow \mathbf{I}$  FOR THE PROPOSED UNSUPERVISED FEATURE LEARNING.

Method	Loss terms		$\mathbf{C} \rightarrow \mathbf{I}$	
	Baseline	$\mathcal{L}_{domain} + \mathcal{L}_{live} + \mathcal{L}_{dis} + \mathcal{L}_{rec}$	HTER↓	AUC↑
IQM-GMM	✓	-	37.77	71.0
[5] (ICB 18)	✓	✓	<b>33.08</b>	<b>75.36</b>
Baweja et al.	✓	-	46.29	48.02
[6] (IJCB 20)	✓	✓	<b>32.13</b>	<b>78.91</b>

TABLE IV  
ABLATION STUDY ON THE PROTOCOL  $\mathbf{C} \rightarrow \mathbf{I}$  FOR THE PROPOSED OOD LIVENESS FEATURE AUGMENTATION.

Module-1 Losses	Loss terms			$\mathbf{C} \rightarrow \mathbf{I}$	
	$\mathcal{L}_{unl} + \mathcal{L}_{pres}$	$\mathcal{L}_{mine}$	$\mathcal{L}_{cs}$	HTER ↓	AUC ↑
✓	-	-	✓	33.57	62.36
✓	✓	-	✓	17.07	88.97
✓	✓	✓	✓	<b>12.43</b>	<b>92.49</b>

TABLE V  
ABLATION STUDY ON THE PROTOCOL  $\mathbf{C} \rightarrow \mathbf{I}$  FOR THE PROPOSED RELIABLE DOMAIN FEATURE AUGMENTATION

Modules 1&2 (basic losses)	Modules		Losses		$\mathbf{C} \rightarrow \mathbf{I}$	
	[12]	$E_{GIN}$	$\mathcal{L}_{adv}$	$\mathcal{L}_d$	HTER ↓	AUC ↑
✓	-	-	-	-	12.43	92.49
✓	✓	-	✓	-	10.50	95.56
✓	-	✓	✓	-	8.00	96.22
✓	-	✓	✓	✓	<b>5.29</b>	<b>98.80</b>

TABLE VI  
COMPARISON OF CROSS-DOMAIN TESTING ON  $[\mathbf{O}, \mathbf{S}] \rightarrow [\mathbf{D}, \mathbf{H}, \mathbf{U}]$ . THE EVALUATION METRICS ARE HTER(%) ↓ AND AUC(%) ↑.

Type	Method	$[\mathbf{O}, \mathbf{S}] \rightarrow \mathbf{D}$		$[\mathbf{O}, \mathbf{S}] \rightarrow \mathbf{H}$		$[\mathbf{O}, \mathbf{S}] \rightarrow \mathbf{U}$	
		HTER	AUC	HTER	AUC	HTER	AUC
2-class	Auxiliary [33]	0.29	99.04	14.64	88.32	37.28	53.14
	NAS [36]	<b>0.22</b>	99.31	15.13	88.91	37.68	<b>72.83</b>
	LDCN [39]	1.49	<b>99.91</b>	<b>8.75</b>	<b>95.60</b>	<b>33.54</b>	60.44
1-class	IQM-GMM [5]	43.83	43.43	19.14	80.53	38.18	66.18
	Baweja et al. [6]	37.86	45.80	35.65	68.90	41.74	49.85
	Lim et al. [8]	27.69	75.47	35.19	62.98	37.34	64.24
	AAE [7]	22.48	78.62	31.22	73.77	45.24	53.48
	OC-SCMNet [16]	1.47	99.87	7.08	86.84	<b>10.61</b>	<b>90.75</b>
	UFDANet (Ours)	<b>1.17</b>	<b>99.92</b>	<b>5.55</b>	<b>96.65</b>	13.76	92.60

these losses. As shown in Table III, models trained with our Module-1 losses demonstrated significant performance improvements on the protocol  $\mathbf{C} \rightarrow \mathbf{I}$  compared to their baseline counterparts. These results indicate that our proposed unsupervised disentangled feature learning losses effectively encourage FAS models to learn disentangled liveness features, even if the original methods were designed with entangled feature learning strategies. This approach reduces the influence of domain information on liveness features and significantly enhances model performance.

2) *Effectiveness of OOD Liveness Feature Augmentation:* To evaluate the effectiveness of the proposed Out-of-Distribution (OOD) liveness feature augmentation, we conducted experiments using different combinations of loss terms based on Module-1: unsupervised disentangled feature learning. Table IV presents the experimental results. The first row of Table IV represents the performance baseline, where the model is trained using: (i) sampled Gaussian noise as pseudo-spoof

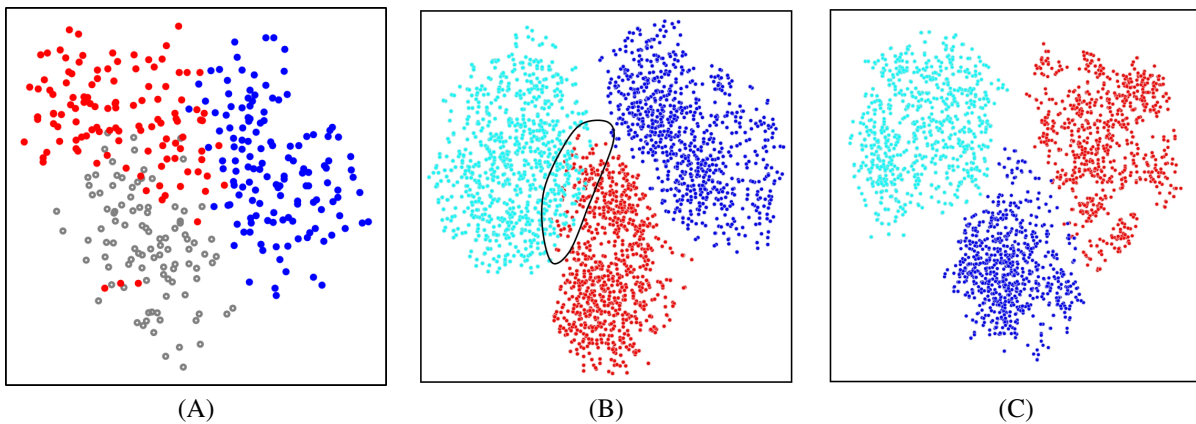


Fig. 8.  $t$ -SNE visualizations of the feature distribution on the protocol  $C \rightarrow I$ . (A) The  $t$ -SNE map of the liveness features. Gray dots represent liveness features from the live class, red dots denote liveness features from the spoof class, and blue dots indicate synthesized OOD liveness features. The visualization demonstrates that the OOD liveness features synthesized by UFDANet effectively extend the live training domain, enhancing generalization to unseen attacks. (B) Domain features synthesized by conventional adversarial domain learning employing only  $\mathcal{L}_{adv}$ . This subfigure shows that although the augmented domain features (cyan) are distant from the original domain features (blue), they distribute near the class boundary and overlap with the liveness features (red), as highlighted by the black contour. Such augmented domain features may interfere with the discriminability of the liveness features. (C) Domain features synthesized using our reliable adversarial domain learning approach with  $\mathcal{L}_{adv} + \mathcal{L}_d$ . This subfigure demonstrates a wider margin between the augmented domain features (cyan), the original domain features (blue), and the liveness features (red), emphasizing the effectiveness of our proposed reliable domain feature augmentation scheme.

features, (ii) the unsupervised disentangled feature learning losses for Module-1 (*i.e.*,  $\mathcal{L}_{live} + \mathcal{L}_{domain} + \mathcal{L}_{dis} + \mathcal{L}_{rec}$ ), and (iii) the cross-entropy loss  $\mathcal{L}_{cs}$ . This baseline performs poorly because Gaussian noise alone cannot sufficiently mimic the liveness features of the spoof class.

Subsequently, we incorporated the OOD liveness feature synthesis loss terms ( $\mathcal{L}_{unl}$  and  $\mathcal{L}_{pres}$ ) to guide the adaptor  $\phi$  in synthesizing OOD liveness features, resulting in significant performance improvements, as shown in the second row of Table IV. Since the model had already learned the liveness features from live images, these losses enabled  $\phi$  to generate latent spoof features divergent from the live class, enhancing the training process. Finally, by introducing the mining loss ( $\mathcal{L}_{mine}$ ), the model achieved the best performance, verifying that  $\mathcal{L}_{mine}$  allows  $\phi$  to explore the latent space more effectively and generate diverse OOD liveness features capable of detecting unseen attacks.

3) *Effectiveness of Reliable Domain Feature Augmentation:* Table V illustrates the performance comparison among different combinations of modules and loss terms developed for domain feature augmentation. The model achieving the best performance in the bottom row of Table IV is considered the baseline for Table V (*i.e.*, the first row of Table V). The table then demonstrates the performance enhancements achieved by incorporating the additional domain feature augmentation module and losses. Table V reveals two key observations. First, under the same adversarial loss  $\mathcal{L}_{adv}$ , our proposed Generative Instance Normalization (GIN) encoder, denoted as  $E_{GIN}$ , outperforms the AdaIN layer [12] in generating unseen domain features. While the AdaIN layer consists of only two learnable parameters and struggles to generate sufficiently diverse domain features, our GIN encoder  $E_{GIN}$  better adapts to unseen domains by sampling a wider range of parameters based on the distribution learned by the condition generator  $G$ . Second,  $\mathcal{L}_d$  further enhances the performance by encouraging  $E_{GIN}$  to synthesize unseen domain features that

closely resemble real-world scenarios.

### C. $t$ -SNE Visualization

1) *Synthesized OOD Liveness Features:* Fig. 8(A) illustrates the distribution of the liveness features extracted from the live faces (gray dots), the liveness features extracted from the spoof faces (red dots), and the synthesized OOD liveness features (blue dots) on the protocol  $C \rightarrow I$ . This figure demonstrates that the synthesized OOD liveness features (blue) not only distribute far away from the live class features (gray), but also scatter widely across regions not covered by the red dots, *i.e.*, the liveness features from the spoof faces, in the latent space. This demonstrates that the OOD liveness features synthesized by UFDANet effectively extend the live training domain, enhancing generalization to unseen attacks.

2) *Augmented Reliable Domain Features:* Fig. 8(B) and Fig. 8(C) visualize different domain features, including the original domain features (blue), the augmented domain features (cyan), and the liveness features (red), under the protocol  $C \rightarrow I$ . Fig. 8(B) shows the visualization results from the experiment corresponding to the third row of Table V. Since the unseen domain features (cyan) in Fig. 8(B) are synthesized solely under the constraint of  $\mathcal{L}_{adv}$ , the augmented domain features near the class boundary exhibit overlap with the liveness features, as highlighted by the black contour. This overlap suggests that the augmented domain features may interfere with the discriminability of the liveness feature. Conversely, with the incorporation of  $\mathcal{L}_d$  (*i.e.*, the bottom row of Table V), Fig. 8(C) demonstrates that the generated domain features (cyan) are farther from the liveness features (red) and closer to the original domain features (blue) compared to Fig. 8(B). This underscores the efficacy of our proposed reliable domain feature augmentation scheme.

TABLE VII  
COMPARISON OF INTRA-DOMAIN FACE PRESENTATION ATTACK DETECTION ON **OULU-NPU**. THE EVALUATION METRICS ARE APCER(%) ↓, BPCER(%) ↓, AND ACER(%) ↓.

Type	Method	P.	APCER	BPCER	ACER	P.	APCER	BPCER	ACER
2-class	CDCN [1] (CVPR 20)	1	0.4	1.7	1.0	2	1.5	1.4	1.5
	CIFL [40] (TIFS 21)		3.8	2.9	3.4		3.6	1.2	2.4
	PatchNet [2] (CVPR 22)		0.0	0.0	<b>0.0</b>		0.8	1.0	0.9
	LDCN [39] (BMVC 22)		0.0	0.0	<b>0.0</b>		0.8	1.0	0.9
	TTN-S [3] (TIFS 22)		0.4	0.0	0.2		0.4	0.8	<b>0.6</b>
1-class	IQM-GMM [5] (ICB 18)	1	75.35	18.56	46.95	2	41.56	27.78	34.67
	Baweja et al. [6] (IJCB 20)		38.63	21.85	30.24		51.81	19.83	35.82
	Lim et al. [8] (Access 20)		43.54	36.5	40.02		72.19	18.5	45.35
	AAE [7] (CCBR 21)		47.13	26.67	36.9		37.28	39.0	38.14
	OC-SCMNet [16] (CVPR 24)		20.83	26.15	23.49		22.05	28.81	25.43
	<b>UFDANet (Ours)</b>		16.38	29.17	<b>22.77</b>		24.72	26.06	<b>25.39</b>
2-class	CDCN [1] (CVPR 20)	3	2.4±1.3	2.2±2.0	2.3±1.4	4	4.6±4.6	9.2±8.0	6.9±2.9
	CIFL [40] (TIFS 21)		3.8±1.3	1.1±1.1	2.5±0.8		5.9±3.3	6.3±4.7	6.1±4.1
	PatchNet [2] (CVPR 22)		1.8±1.47	0.56±1.24	1.18±1.26		2.5±3.81	3.33±3.73	2.90±3.00
	LDCN [39] (BMVC 22)		4.55±4.55	0.58±0.91	2.57±2.67		4.50±1.48	3.17±3.49	3.83±2.12
	TTN-S [3] (TIFS 22)		1.0±1.1	0.8±1.3	<b>0.9±0.7</b>		3.3±2.8	2.5±2.0	<b>2.9±1.4</b>
1-class	IQM-GMM [5] (ICB 18)	3	57.17±16.79	16.5±6.95	36.83±5.35	4	53.42±14.08	16.67±8.38	35.04±3.95
	Baweja et al. [6] (IJCB 20)		45.39±12.82	18.28±16.21	31.83±6.99		60.25±16.49	10.67±10.37	35.46±5.43
	Lim et al. [8] (Access 20)		38.51±13.08	39.52±11.13	39.02±2.16		36.91±10.24	20.5±8.01	28.07±5.32
	AAE [7] (CCBR 21)		26.62±13.67	52.93±16.09	39.77±3.74		26.33±18.5	40.17±29.04	33.12±8.9
	OC-SCMNet [16] (CVPR 24)		27.10±12.57	20.55±11.12	23.83±3.14		16.41±14.00	11.66±9.42	14.04±4.90
	<b>UFDANet (Ours)</b>		19.04±8.94	21.33±7.09	<b>20.19±3.47</b>		4.08±3.29	6.83±9.06	<b>5.46±5.30</b>



Fig. 9. Illustration of live images (boxes in green) and spoof images (boxes in red), along with their respective activation maps for each category.

### D. Activation Visualization

In Figure 9, we visualize the activation maps on the cross-domain protocol  $[O, S] \rightarrow [D, H, U]$ , which involves 3D mask attacks. First, we see that the activation maps of live images primarily concentrate on facial regions, with even the forehead showing relatively high responses. Next, the spoof activation maps of 3D mask attacks concentrate mainly on the 3D facial masks, without extending to the forehead of the real face. From these visualization results, we see that the proposed UFDANET effectively focuses on the crucial regions to capture spoof cues and learn discriminative features, enabling it to distinguish real faces from spoofed ones.

### E. Intra-Domain and Cross-Domain Testings

This section presents a comprehensive comparison of detection performance and model generalization capability between UFDANet, recent two-class FAS methods [1]–[3], [11], [15], [33], [36], [37], [39]–[43], and recent one-class FAS methods [5]–[8], [16], evaluated through extensive intra-domain and cross-domain testings.

1) *Intra-Domain Testing*: Table VII demonstrates that the proposed UFDANet, as a one-class approach, achieves a significant advantage over all other one-class FAS methods in the intra-domain testing scenario on OULU-NPU [30].

TABLE VIII  
COMPARISON OF CROSS-DOMAIN TESTING ON  $[M, I] \rightarrow C$  AND  $[M, I] \rightarrow O$ . THE EVALUATION METRICS ARE HTER(%) ↓ AND AUC(%) ↑.

Type	Method	$[M, I] \rightarrow C$		$[M, I] \rightarrow O$	
		HTER	AUC	HTER	AUC
2-class	MADDG [37] (CVPR 19)	41.02	64.33	39.35	65.10
	SSDG-M [15] (CVPR 20)	31.89	71.29	36.01	66.88
	SDA [42] (AAAI 21)	32.17	72.79	28.90	73.33
	SSAN-M [11] (CVPR 22)	30.00	76.20	29.44	76.62
	LDCN [39] (BMVC 22)	22.22	82.87	21.54	86.06
	CADMA [14] (ICASSP 22)	28.75	75.78	26.28	80.46
	DiVT-M [43] (WACV 23)	<b>20.11</b>	<b>86.71</b>	23.61	85.73
	NDA-FAS [4] (TIFS 23)	21.78	83.01	21.41	86.35
DFANet [12] (ICME 23)	20.67	84.87	<b>18.61</b>	<b>89.52</b>	
1-class	IQM-GMM [5] (ICB 18)	45.81	39.74	35.0	37.01
	Baweja et al. [6] (IJCB 20)	27.33	78.50	32.01	72.19
	Lim et al. [8] (Access 20)	43.56	53.6	39.19	64.11
	AAE [7] (CCBR 21)	46.67	47.28	48.52	47.99
	OC-SCMNet [16] (CVPR 24)	21.67	<b>85.30</b>	22.03	<b>84.28</b>
	<b>UFDANet (Ours)</b>	<b>21.66</b>	82.42	<b>21.92</b>	82.84

In this scenario, because spoof attacks share highly similar characteristics between the training and testing data, two-class FAS methods are better at distinguishing between live and spoof features, significantly outperforming one-class methods. However, despite being a one-class FAS method, UFDANet substantially narrows the performance gap with two-class methods, underscoring the effectiveness of its unsupervised feature disentanglement and OOD liveness feature adaptation modules.

2) *Cross-Domain Testing*: Tables VIII, IX, and VI present cross-domain testing results evaluating the generalization capability of the proposed UFDANet.

Table VIII presents the cross-domain testing results based on the settings in [37] for the protocols  $[M, I] \rightarrow C$  and  $[M, I] \rightarrow O$ , designed to detect print and replay attacks. As described in [37], datasets **M** and **I** are used for model training due to their substantial domain variation, while datasets **C** and **O** are reserved for testing. In Table VIII, UFDANet outperforms all one-class FAS methods in terms of HTER while achieving

TABLE IX  
COMPARISON OF CROSS-DOMAIN TESTING ON  $\mathbf{C} \rightarrow \mathbf{I}$  AND  $\mathbf{I} \rightarrow \mathbf{C}$ . THE EVALUATION METRIC IS HTER(%)  $\downarrow$ .

Type	Method	$\mathbf{C} \rightarrow \mathbf{I}$	$\mathbf{I} \rightarrow \mathbf{C}$
2-class	Auxiliary [33] (CVPR 18)	27.6	28.4
	STASN [41] (CVPR 19)	31.5	30.9
	CDCN [1] (CVPR 20)	15.5	32.6
	CIFL [40] (TIFS 21)	17.6	-
	PatchNet [2] (CVPR 22)	<b>9.9</b>	<b>26.2</b>
	NDA-FAS [4] (TIFS 23)	12.5	31.2
1-class	IQM-GMM [5] (ICB 18)	31.93	48.44
	Baweja <i>et al.</i> [6] (IJCB 20)	46.29	29.44
	Lim <i>et al.</i> [8] (Access 20)	37.36	39.78
	AAE [7] (CCBR 21)	20.0	26.9
	OC-SCMNet [16] (CVPR 24)	7.29	17.44
	<b>UFDANet (Ours)</b>	<b>5.29</b>	<b>17.43</b>

competitive performance compared to two-class FAS methods. This result suggests that two-class FAS methods may overfit the training data, leading to significant performance degradation on unseen domains due to cross-domain shifts in spoofing characteristics. In contrast, the proposed **UFDANet** operates without prior knowledge of the spoof class, demonstrating superior domain generalization ability in detecting unseen spoof attacks in cross-domain testing scenarios.

Following the experimental configurations in [33], we conducted cross-domain tests on the datasets  $\mathbf{C}$  and  $\mathbf{I}$ , as shown in Table IX. Dataset  $\mathbf{C}$  contains both high- and low-resolution data, whereas dataset  $\mathbf{I}$  consists solely of low-resolution data. Consequently, the protocol  $\mathbf{I} \rightarrow \mathbf{C}$  is inherently more challenging than  $\mathbf{C} \rightarrow \mathbf{I}$ , as models trained exclusively on low-resolution data often struggle to generalize to high-resolution data—a persistent challenge for two-class FAS methods. In contrast, as a one-class FAS method, **UFDANet** significantly improves detection performance and even outperforms two-class FAS methods in this scenario. These results highlight the effectiveness of **UFDANet** in cross-domain testing.

Finally, we followed the experimental settings in [36] to perform cross-domain testing on 3D-mask attack types, with results detailed in Table VI. Our model was trained on live images from datasets  $\mathbf{O}$  and  $\mathbf{S}$  and tested on datasets  $\mathbf{D}$ ,  $\mathbf{H}$ , and  $\mathbf{U}$ .

Two-class FAS methods, typically trained on live images and spoof images with print and replay attacks, often struggle to generalize to previously unseen attacks such as 3D-mask attacks, as observed in the  $[\mathbf{O}, \mathbf{S}] \rightarrow \mathbf{U}$  protocol. In contrast, **UFDANet** outperforms all FAS methods, including both one-class and two-class approaches, on the  $[\mathbf{O}, \mathbf{S}] \rightarrow \mathbf{U}$  and  $[\mathbf{O}, \mathbf{S}] \rightarrow \mathbf{H}$  protocols. Additionally, **UFDANet** achieves competitive performance against two-class methods on the  $[\mathbf{O}, \mathbf{S}] \rightarrow \mathbf{D}$  protocol. These results further demonstrate the efficacy of the proposed **UFDANet** in handling cross-domain scenarios.

## V. CONCLUSION

In this paper, we introduced a novel Unsupervised Feature Disentanglement and Augmentation Network (**UFDANet**) to tackle the challenges of one-class Face Anti-Spoofing (FAS). Recognizing that one-class FAS models often struggle with overfitting and domain sensitivity due to entangled liveness

features, we proposed a new unsupervised feature disentanglement approach that effectively separates liveness and domain features. This disentanglement facilitates more discriminative liveness feature learning. To further enhance the model’s ability to represent and detect spoof attempts, we incorporated an innovative liveness feature augmentation scheme, designed to generate liveness features that deviate from the live class, simulating unseen spoof attacks. Additionally, to improve the generalizability of the model across different domains, we introduced a domain feature augmentation routine, enabling the synthesis of reliable unseen domain features. Extensive experiments demonstrate that **UFDANet** not only significantly outperforms previous one-class FAS methods but also achieves competitive performance compared to state-of-the-art two-class FAS models. These results validate the effectiveness of our approach in enhancing the representability, discriminability, and generalization capability of one-class FAS systems.

## REFERENCES

- [1] Z. Yu, C. Zhao, Z. Wang, Y. Qin, Z. Su, X. Li, F. Zhou, and G. Zhao, “Searching central difference convolutional networks for face anti-spoofing,” in *Proc. IEEE/CVF Conf. Comput. Vis. Pattern Recog.*, 2020, pp. 5295–5305.
- [2] C. Wang, Y. Lu, S. Yang, and S. Lai, “Patchnet: A simple face anti-spoofing framework via fine-grained patch recognition,” in *Proc. IEEE/CVF Conf. Comput. Vis. Pattern Recog.*, 2022, pp. 20281–20290.
- [3] Z. Wang, Q. Wang, W. Deng, and G. Guo, “Learning multi-granularity temporal characteristics for face anti-spoofing,” *IEEE Trans. Inf. Forensics Secur.*, vol. 17, pp. 1254–1269, 2022.
- [4] W. Wang, P. Liu, H. Zheng, R. Ying, and F. Wen, “Domain generalization for face anti-spoofing via negative data augmentation,” *IEEE Trans. Inf. Forensics Secur.*, vol. 18, pp. 2333–2344, 2023.
- [5] O. Nikisins, A. Mohammadi, A. Anjos, and S. Marcel, “On effectiveness of anomaly detection approaches against unseen presentation attacks in face anti-spoofing,” in *Proc. Int. Conf. Biometrics*, 2018, pp. 75–81.
- [6] Y. Baweja, P. Oza, P. Perera, and V. Patel, “Anomaly detection-based unknown face presentation attack detection,” in *Proc. IEEE Int. Joint Conf. Biometrics*, 2020, pp. 1–9.
- [7] X. Huang, J. Xia, and L. Shen, “One-class face anti-spoofing based on attention auto-encoder,” in *Proc. 15th Chin Conf. Biometric Recognit.*, 2021, pp. 365–373.
- [8] S. Lim, Y. Gwak, W. Kim, J. Roh, and S. Cho, “One-class learning method based on live correlation loss for face anti-spoofing,” *IEEE Access*, vol. 8, pp. 201635–201648, 2020.
- [9] K. Zhang, T. Yao, J. Zhang, Y. Tai, S. Ding, J. Li, F. Huang, H. Song, and L. Ma, “Face anti-spoofing via disentangled representation learning,” in *Proc. European Conf. Comput. Vis.*, 2020, pp. 641–657.
- [10] G. Wang, H. Han, S. Shan, and X. Chen, “Cross-domain face presentation attack detection via multi-domain disentangled representation learning,” in *Proc. IEEE/CVF Conf. Comput. Vis. Pattern Recog.*, 2020, pp. 6678–6687.
- [11] Z. Wang, Z. Wang, Z. Yu, W. Deng, J. Li, T. Gao, and Z. Wang, “Domain generalization via shuffled style assembly for face anti-spoofing,” in *Proc. IEEE/CVF Conf. Comput. Vis. Pattern Recog.*, 2022, pp. 4123–4133.
- [12] P. Huang, J. Chong, H. Ni, T. Chen, and C. Hsu, “Towards diverse liveness feature representation and domain expansion for cross-domain face anti-spoofing,” in *Proc. IEEE Int. Conf. Multimedia Expo.*, 2023, pp. 1199–1204.
- [13] H. Wu, D. Zeng, Y. Hu, H. Shi, and T. Mei, “Dual spoof disentanglement generation for face anti-spoofing with depth uncertainty learning,” *IEEE Trans. Circuits Syst. Video Technol.*, vol. 32, no. 7, pp. 4626–4638, 2022.
- [14] H. Huang, Y. Xiang, G. Yang, L. Lv, X. Li, Z. Weng, and Y. Fu, “Generalized face anti-spoofing via cross-adversarial disentanglement with mixing augmentation,” in *Proc. IEEE Int. Conf. Acoust. Speech Signal Process.*, 2022, pp. 2939–2943.
- [15] Y. Jia, J. Zhang, S. Shan, and X. Chen, “Single-side domain generalization for face anti-spoofing,” in *Proc. IEEE/CVF Conf. Comput. Vis. Pattern Recog.*, 2020, pp. 8484–8493.

- [16] P.-K. Huang, C.-H. Chiang, T.-H. Chen, J.-X. Chong, T.-L. Liu, and C.-T. Hsu, "One-class face anti-spoofing via spoof cue map-guided feature learning," in *Proceedings of the IEEE/CVF Conference on Computer Vision and Pattern Recognition*, 2024.
- [17] C. Tsai, T. Wu, and S. Lai, "Multi-scale patch-based representation learning for image anomaly detection and segmentation," in *Proc. IEEE/CVF Winter Conf. Appl. Comput. Vis.*, 2022, pp. 3992–4000.
- [18] J. Hyun, S. Kim, G. Jeon, S. Kim, K. Bae, and B. Kang, "Reconpatch: Contrastive patch representation learning for industrial anomaly detection," *arXiv:2305.16713*, 2023.
- [19] E. Nowara, D. McDuff, and A. Veeraraghavan, "The benefit of distraction: Denoising camera-based physiological measurements using inverse attention," in *Proc. IEEE/CVF Int. Conf. Comput. Vis.*, 2021, pp. 4955–4964.
- [20] Z. Sun and X. Li, "Contrast-phys: Unsupervised video-based remote physiological measurement via spatiotemporal contrast," in *Proc. European Conf. Comput. Vis.*, 2022, pp. 492–510.
- [21] H. Yue, K. Wang, G. Zhang, H. Feng, J. Han, E. Ding, and J. Wang, "Cyclically disentangled feature translation for face anti-spoofing," in *Proceedings of the AAAI conference on artificial intelligence*, vol. 37, no. 3, 2023, pp. 3358–3366.
- [22] H.-C. Shao, K.-Y. Liu, W.-T. Su, C.-W. Lin, and J. Lu, "Dotfan: a domain-transferred face augmentation net," *IEEE Trans. Image Process.*, vol. 30, pp. 8759–8772, 2021.
- [23] D. Wen, H. Han, and A. Jain, "Face spoof detection with image distortion analysis," *IEEE Trans. Inf. Forensics Secur.*, vol. 10, no. 4, pp. 746–761, 2015.
- [24] I. Standard, "Information technology—biometric presentation attack detection—part 1: Framework," *ISO: Geneva, Switzerland*, 2016.
- [25] P. Huang, C. Chang, H. Ni, and C. Hsu, "Learning to augment face presentation attack dataset via disentangled feature learning from limited spoof data," in *Proc. IEEE Int. Conf. Multimedia Expo*, 2022, pp. 1–6.
- [26] Z. Yu, X. Li, X. Niu, J. Shi, and G. Zhao, "Face anti-spoofing with human material perception," in *Computer Vision—ECCV 2020: 16th European Conference, Glasgow, UK, August 23–28, 2020, Proceedings, Part VII 16*. Springer, 2020, pp. 557–575.
- [27] H.-Y. Tseng, H. Lee, J. Huang, and M. Yang, "Cross-domain few-shot classification via learned feature-wise transformation," in *ICLR*, 2020.
- [28] X. Huang and S. Belongie, "Arbitrary style transfer in real-time with adaptive instance normalization," in *Proc. IEEE/CVF Int. Conf. Comput. Vis.*, 2017, pp. 1510–1519.
- [29] W. Youden, "Index for rating diagnostic tests," *Cancer*, vol. 3, no. 1, pp. 32–35, 1950.
- [30] Z. Boulkenafet, J. Komulainen, L. Li, X. Feng, and A. Hadid, "Oulu-npu: A mobile face presentation attack database with real-world variations," in *Proc. IEEE Int. Conf. Autom. Face Gesture Recognit.*, 2017, pp. 612–618.
- [31] Z. Zhang, J. Yan, S. Liu, Z. Lei, D. Yi, and S. Li, "A face antispoofing database with diverse attacks," in *Proc. Int. Conf. Biometrics*, 2012, pp. 26–31.
- [32] I. Chingovska, A. Anjos, and S. Marcel, "On the effectiveness of local binary patterns in face anti-spoofing," in *Proc. Int. Conf. Biometrics Special Interest Group*, 2012, pp. 1–7.
- [33] Y. Liu, A. Jourabloo, and X. Liu, "Learning deep models for face anti-spoofing: Binary or auxiliary supervision," in *Proc. IEEE/CVF Conf. Comput. Vis. Pattern Recog.*, 2018, pp. 389–398.
- [34] N. Erdogmus and S. Marcel, "Spoofing face recognition with 3d masks," *IEEE Trans. Inf. Forensics Secur.*, vol. 9, no. 7, pp. 1084–1097, 2014.
- [35] S. Liu, P. Yuen, S. Zhang, and G. Zhao, "3d mask face anti-spoofing with remote photoplethysmography," in *Proc. European Conf. Comput. Vis.*, 2016, pp. 85–100.
- [36] Z. Yu, J. Wan, Y. Qin, X. Li, S. Li, and G. Zhao, "Nas-fas: Static-dynamic central difference network search for face anti-spoofing," *IEEE Trans. Pattern Anal. Mach. Intell.*, vol. 43, no. 9, pp. 3005–3023, 2020.
- [37] R. Shao, X. Lan, J. Li, and P. Yuen, "Multi-adversarial discriminative deep domain generalization for face presentation attack detection," in *Proc. IEEE/CVF Conf. Comput. Vis. Pattern Recog.*, 2019, pp. 10023–10031.
- [38] A. Anjos and S. Marcel, "Counter-measures to photo attacks in face recognition: a public database and a baseline," in *Proc. IEEE Int. Joint Conf. Biometrics*, 2011, pp. 1–7.
- [39] P. Huang, H. Ni, Y. Ni, and C. Hsu, "Learnable descriptive convolutional network for face anti-spoofing," in *Proc. 33rd Brit. Mach. Vis. Conf.*, 2022, p. 239.
- [40] B. Chen, W. Yang, H. Li, S. Wang, and S. Kwong, "Camera invariant feature learning for generalized face anti-spoofing," *IEEE Trans. Inf. Forensics Secur.*, vol. 16, pp. 2477–2492, 2021.
- [41] X. Yang, W. Luo, L. Bao, Y. Gao, D. Gong, S. Zheng, Z. Li, and W. Liu, "Face anti-spoofing: Model matters, so does data," in *Proc. IEEE/CVF Conf. Comput. Vis. Pattern Recog.*, 2019, pp. 3507–3516.
- [42] J. Wang, J. Zhang, Y. Bian, Y. Cai, C. Wang, and S. Pu, "Self-domain adaptation for face anti-spoofing," in *Proc. 35rd AAAI Conf. Artif. Intell.*, 2021, pp. 2746–2754.
- [43] C. Liao, W. Chen, H. Liu, Y. Yeh, M. Hu, and C. Chen, "Domain invariant vision transformer learning for face anti-spoofing," in *Proc. IEEE/CVF Winter Conf. Appl. Comput. Vis.*, 2023, pp. 6098–6107.